ChemComm

ROYAL SOCIETY OF CHEMISTRY

COMMUNICATION

View Article Online
View Journal | View Issue

Synthesis of a tetrabenzotriazacorrole μ-oxo dimer and investigation of its stacking effect†

Cite this: *Chem. Commun.*, 2014, **50**, 4312

Received 12th February 2014,
Accepted 25th February 2014

DOI: 10.1039/c4cc01115e

www.rsc.org/chemcomm

Taniyuki Furuyama, Yusuke Sugiya and Nagao Kobayashi*

A μ-oxo dimer of phosphorus(V) tetrabenzotriazacorrole (PTBC) has been synthesized and characterized for the first time. Spectroscopic and theoretical analysis support the opinion that two PTBC chromophore groups interact with each other, while the low-symmetric PTBC structure is also efficient for generating singlet oxygen.

Phthalocyanines (Pcs) and related tetrapyrrolic macrocycles are attractive target molecules in a variety of fields. These molecules have intense absorption bands in the UV-visible region, and their unique optical properties can be used as a key characteristic for constructing functional molecules. Since the optical properties of Pcs depend significantly on their structure, a number of Pc derivatives have been proposed and synthesized for over a century.[1] Among several methods in this regard, lowering of the molecular symmetry of Pcs is a good strategy.[2] However, separation of low-symmetry Pcs is generally not easy, and the yield is often low. Properties resulting from aggregation and/or oligomerization of Pcs are also important in various fields, such as materials science and photochemistry.[3] We focus on tetrabenzotriazacorrole (TBC) as a variant of low-symmetry Pcs. TBC is known as a 18π aromatic Pc–corrole analogue, in which one *meso* nitrogen atom of Pc is missing. The direct pyrrole–pyrrole bond results in reduced symmetry (C_{2v}) compared to the D_{4h} of regular metallo Pcs. TBCs can be synthesized from the corresponding symmetric Pcs in moderate yields by using a simple procedure, and are easy to handle.[4] In order to learn more about TBCs, we have chosen phosphorus(V) complexes which have two axial ligands.[4a,c] Herein, we report the first synthesis and properties of a TBC μ-oxo dimer as a cofacial model of low-symmetry Pc oligomers. μ-oxo oligomers have been synthesized in Pc chemistry, and unique stacking effects observed.[5]

The synthetic route of the TBC μ-oxo dimer (**4**) is shown in Scheme 1a. Free-base β-$(PhO)_8$Pc **1** was reacted with excess phosphorus tribromide in pyridine, to give the TBC phosphorus complex **2**. The reaction was quenched with water, and the axial ligands of **2** were OH at this stage. The solution of **2** was heated in the presence of triphenylsilyl chloride, and both the triphenylsiloxy-capped TBC monomer **3** and the desired dimer **4** were obtained. The bulkiness of the triphenylsilyl group appeared efficient for stabilization of the dimer. The structure of **3** was finally elucidated by X-ray diffraction analysis of crystals (Scheme 1b and Fig. S1, ESI†).‡ The TBC macrocycle of **3** has a highly planar structure as previously reported for phosphorus(V) corrolazine[4c] and corrole[6] complexes. The phosphorus ion is just the right size to fit into the center of the TBC ligand, while phosphorus(V) Pc has a ruffled structure[7] due to mismatching between phosphorus and a central core of Pc.

^{1}H and ^{31}P NMR spectra of **3** and **4** in $CDCl_3$ are shown in Fig. S2 (ESI†). Four sets of singlet assignable to the α-position of **3** are present at low magnetic field (9.11–9.02 and 8.34 ppm), reflecting the lower-symmetric TBC macrocycle. The ^{31}P NMR spectrum of **3** exhibits only one peak, at −216 ppm, similar to porphyrin[8] and

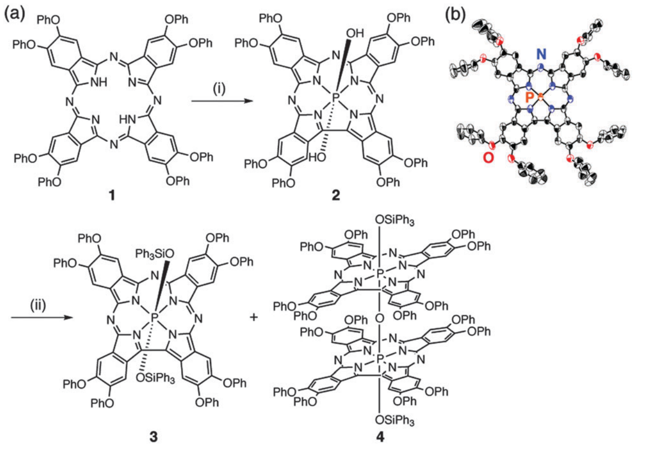

Scheme 1 (a) Synthesis of the tetrabenzotriazacorrole μ-oxo dimer. *Reagents and conditions*: (i) PBr_3 (20 eq.), pyridine, reflux, 1 h, 55%; (ii) Ph_3SiCl, toluene, reflux, 3 h in the dark, 60% (**3**) and 3% (**4**). (b) The X-ray crystal structure of **3**. The thermal ellipsoids were scaled to the 50% probability level. H atoms and axial ligands have been omitted for clarity.

Department of Chemistry, Graduate School of Science, Tohoku University, Sendai 980-8578, Japan. E-mail: nagaok@m.tohoku.ac.jp; Tel: +81 22 795 7719

† Electronic supplementary information (ESI) available: Additional spectroscopic data and full details of experimental and calculation procedures for all studied compounds. CCDC 985980. For ESI and crystallographic data in CIF or other electronic format see DOI: 10.1039/c4cc01115e

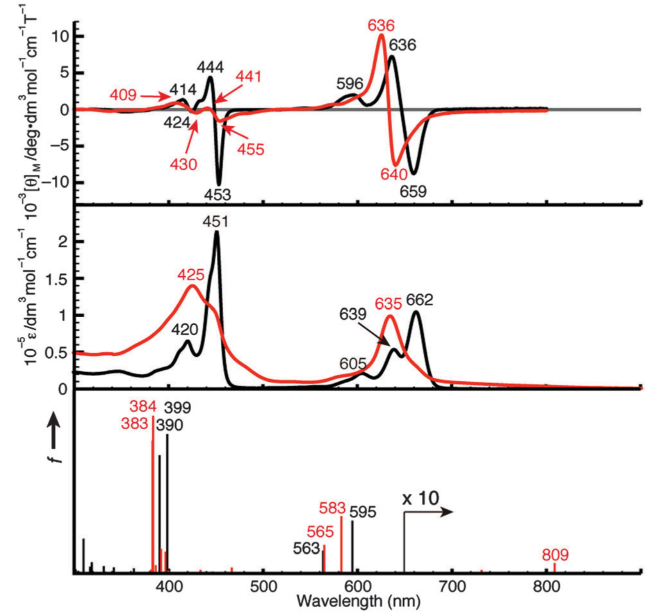

Fig. 1 Magnetic circular dichroism (top), and electronic absorption (middle) spectra of **3** (black) and **4** (red) in $CHCl_3$, and theoretical absorption spectra (bottom) of **3′** (black) and **4′** (red). Calculations were carried out at the B3LYP/6-31G(d) level of theory.

phthalocyanine[7] phosphorus(V) complexes. Both ^{1}H and ^{31}P NMR spectra of **4** exhibit only one set of peaks for the TBC unit, and each TBC moiety could not be distinguished even at low temperature (Fig. S3, ESI†). The peaks of **4** were observed at higher field than those of **3**. A similar upfield shift was also observed in the case of the μ-oxo dimer of SiPc,[5c] indicating that each TBC moiety is affected by the diatropic ring current generated in the other TBC moiety.

UV-vis and MCD spectra of compounds **3** and **4** in $CHCl_3$ are shown in Fig. 1. The absorption spectrum of capped monomer **3** exhibits two intense bands at 662 nm and 451 nm for the Q and Soret bands, respectively. Both the absorption coefficients and positions of the Q and Soret bands are close to those of the spectrum of **2** (Fig. S4, ESI†). In the MCD spectrum, pseudo Faraday *A* terms of almost comparative intensity appeared corresponding to the Q and Soret absorption bands. On the other hand, the absorption spectrum of dimer **4** is completely different from that of **3**. Here, the absorption bands are blue-shifted to 635 and 425 nm with concomitant broadening, although the apparent intensity is close to that of the monomer. In the near-IR region (680–800 nm), a weak, broad band, monotonously decreasing toward a longer wavelength, is seen, suggesting the presence of a low-energy forbidden transition for the dimer. In the MCD spectrum, an intense pseudo Faraday *A* term appeared, corresponding to the Q absorption peak, indicating that the MCD spectrum of cofacial dimers does not sensitively reflect the molecular symmetry of the constituent monomer.

The electrochemical properties of **3** and **4** were examined by cyclic voltammetry (Fig. 2). **3** showed one reversible oxidation couple at 0.19 V, while **4** showed two reversible oxidation couples at 0.44 and −0.02 V *vs.* Fc$^+$/Fc. The first oxidation couple (E_{ox1}) shifted cathodically by *ca.* 0.2 V compared to that of the monomer **3**. Since the exact reduction potentials could not be estimated, their cathodic peak potentials, E_{pc}, were used as indexes of the first reduction potential. The close E_{pc} values clearly show that the LUMO energy levels of **3** and **4** are close. These voltammograms indicate that the gap between the HOMO and the LUMO decreases after the μ-oxo dimer formation of the TBC macrocycle.

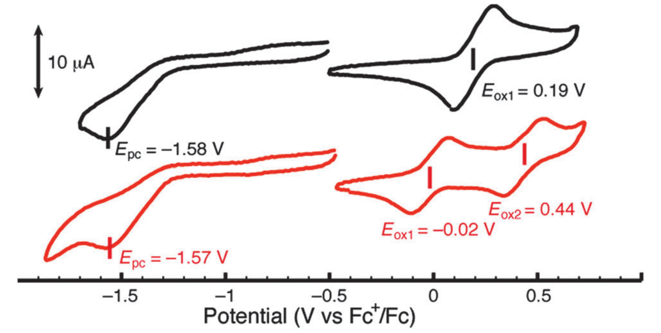

Fig. 2 Cyclic voltammetry data for **3** (black), and **4** (red). Cyclic voltammograms were acquired from 1.0 mM solutions of an analyte in 0.1 M ^{n}Bu$_4$NClO$_4$/*o*-DCB. Ferrocene was used as an internal standard and set to 0 V.

In order to enhance the interpretation of the electronic structure of the TBC μ-oxo dimer and understand the origin of the blue-shifted absorption spectrum of **4** with a narrower energy gap compared to that of monomer **3**, model structures (**3′** and **4′**), whose peripheral substituents and axial triphenylsilyl groups are replaced by hydrogen, were considered and used in the calculations. The torsion angle (θ) of the optimized structure of **4′** is 41.4° (Fig. S5, ESI†), which is larger than that of the crystallographic structure of the μ-oxo SiPc dimer (θ = 36.6°).[5e] The optimized structures where θ was restricted were also obtained, but their energy difference was smaller than 4 kcal mol^{-1} (Fig. S6, ESI†), thus allowing for the two TBC macrocycles to undergo a rapid rotation, supporting the variable temperature ^{1}H NMR results.

The calculated absorption spectra of **3′** and **4′** are shown at the bottom of Fig. 1, while partial MO energy diagrams are shown in Fig. S7 (ESI†), with the calculated transition energies, oscillator strengths (*f*), and configurations summarized in Table S1 (ESI†). As previously reported for the electronic structure of silicon(IV) corrolazine,[9] the absorption spectrum of monomer **3′** can be explained by Gouterman's "four-orbital" theory.[10] Both the calculated Q and Soret bands split into two due to the low-symmetry of the TBC chromophore. These bands are composed of transitions from the HOMO − 1 and HOMO to the LUMO and LUMO + 1, similar to typical aromatic azaporphyrinoids. The frontier MOs of μ-oxo dimeric **4′** are delocalized over the entire complex. Here, the HOMO–LUMO gap of **4′** (1.93 eV) is narrower than that of **3′** (2.28 eV). On the other hand, the calculated HOMO–LUMO transition at 809 nm is very weak (*f* = 0.01). The main Q bands calculated at 583 and 565 nm are relatively strong, and the sum of the two *f* values (0.46) are close to that (0.41) of the calculated Q band for monomeric **3′** (595 and 563 nm), as is indeed observed experimentally for **3** and **4**. Based on the components of transitions for **4′**, the lowest-energy transition is forbidden, and the HOMO − 3, HOMO − 2, and HOMO − 1 dominate in the intense Q absorption band for **4′**. Therefore, the transition component of the intense band in the Q band region of **4** is completely different from that of **3**, as a result of the

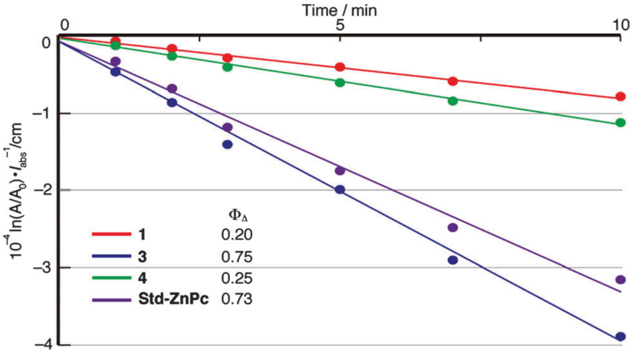

Fig. 3 Comparison of the rate of decay of DPBF sensitized by **1** (red), **3** (blue), **4** (green) and **Std-ZnPc** (purple) in $CHCl_3$ as shown by the decrease in the absorbance at 415 nm. The absorption coefficient was normalized by the rates of the light absorption coefficient over 600 nm.

orbital interaction between the two TBC chromophores. These spectroscopic features can also be interpreted conceptually by considering exciton coupling interactions between the co-facially arranged monomer units (H-type aggregate).[11] In the dimer, the orientation of two excitons derived from the monomer units is not perfectly parallel. However, as a first approximation, the band on the lower energy side of the Q band can be expressed as the difference of two electric dipole moments, and that on the higher energy side as the sum of the two moments; thus the band at higher energy becomes much stronger.

Finally, we demonstrate the photosensitising efficiency of TBCs[12] by determining their singlet oxygen quantum yields (Φ_Δ) by a steady-state method using 1,3-diphenylisobenzofuran (DPBF) as the chemical quencher. A β-(4-*t*-BuOPh)$_8$Pc zinc complex (**Std-ZnPc**) was used as a standard (Φ_Δ = 0.73 in $CHCl_3$).[13] The photobleaching decays are shown in Fig. 3. TBC monomer **3** showed a high quantum yield (Φ_Δ = 0.75), while free-base Pc had a low Φ_Δ value. Compound **3** consists only of main-group elements above the third period, and therefore, its high Φ_Δ value is considered not to be caused by a heavy-metal effect, but due to the low-symmetry chromophore[14] of TBC. On the other hand, dimer **4** (Φ_Δ = 0.25) was much less efficient than **3**. In general, H-type aggregation in water reduces the lifetime of the excited state due to enhanced radiationless excited-state dissipation.[15]

In summary, a μ-oxo phosphorus(V) TBC dimer has been synthesized for the first time. In accordance with the narrower HOMO–LUMO gap derived from cyclic voltammograms, the dimer showed a weak Q absorption band with a forbidden character at a longer wavelength than the Q band of the monomer. The strong band of the dimer was observed to be blue-shifted than that of the constituting monomer. These spectral features could be explained by theoretical calculations, and conceptually by an exciton coupling model. The low-symmetry structure of TBC showed enhanced efficiency in generating singlet oxygen, so that the molecular symmetry appears to be important in the design of sensitizers. Further work is currently underway to tune the rotation properties by external stimuli.

This work was partly supported by a Grant-in-Aids for Scientific Research on Innovative Areas (25109502, ''Stimuli-responsive Chemical Species''), Scientific Research (B) (No. 23350095), Challenging Exploratory Research (No. 25620019) and Young Scientist (B) (No. 24750031) from the Ministry of Education, Culture, Sports, Science, and Technology (MEXT). The authors thank Dr Eunsang Kwon (Tohoku University) for X-ray measurements. Some of the calculations were performed using supercomputing resources at the Cyberscience Center of Tohoku University.

Notes and references

‡ Crystallographic data for **3**: $C_{116}H_{78}N_7O_{10}PSi_2$, M_w = 1817.00, orthorhombic, space group *Pbca* (no. 61), a = 12.5583(2) Å, b = 31.0602(6) Å, c = 47.1556(8) Å, V = 18393.7(6) Å^3, Z = 8, ρ_{calcd} = 1.312 g cm^{-3}, T = −183 °C, 202 162 measured reflections, 16 834 unique reflections (R_{int} = 0.0934), R = 0.0974 ($I > 2\sigma(I)$), R_w = 0.3134 (all data), goodness-of-fit on F^2 = 1.035, largest diff. peak/hole 1.007 and −0.317 e Å^{-3}, CCDC 985980.

1 (*a*) *The Porphyrin Handbook*, ed. K. M. Kadish, K. M. Smith and R. Guilard, Academic Press, San Diego, United States, 2003; (*b*) *Handbook of Porphyrin Science*, ed. K. M. Kadish, K. M. Smith and R. Guilard, World Scientific Publishing, Singapore, 2010.
2 (*a*) J. Mack and N. Kobayashi, *Chem. Rev.*, 2011, **111**, 281; (*b*) J.-J. Cid, M. Garcia-Iglesias, J.-H. Yum, A. Forneli, J. Albero, E. Martínez-Ferrero, P. Vázquez, M. K. Nazeeruddin, E. Palomares and T. Torres, *Chem.–Eur. J.*, 2009, **15**, 5130.
3 (*a*) T. Fukuda, K. Matsumura and N. Ishikawa, *J. Phys. Chem. A*, 2013, **117**, 10447; (*b*) M. García-Iglesias, K. Peuntinger, A. Kahnt, J. Krausmann, P. Vázquez, D. González-Rodríguez, D. M. Guldi and T. Torres, *J. Am. Chem. Soc.*, 2013, **135**, 19311; (*c*) I. Sánchez-Molina, C. G. Claessens, B. Grimm, D. M. Guldi and T. Torres, *Chem. Sci.*, 2013, **4**, 1338.
4 (*a*) J. P. Fox and D. P. Goldberg, *Inorg. Chem.*, 2003, **42**, 8181; (*b*) N. Kobayashi, F. Furuya, G.-C. Yug, H. Wakita, M. Yokomizo and N. Ishikawa, *Chem.–Eur. J.*, 2002, **8**, 1474; (*c*) B. Ramdhanie, C. L. Stern and D. P. Goldberg, *J. Am. Chem. Soc.*, 2001, **123**, 9447; (*d*) J. Li, L. R. Subramanian and M. Hanack, *Chem. Commun.*, 1997, 679; (*e*) M. Fujiki, H. Tabei and K. Isa, *J. Am. Chem. Soc.*, 1986, **108**, 1532.
5 (*a*) K. Oniwa, S. Shimizu, Y. Shiina, T. Fukuda and N. Kobayashi, *Chem. Commun.*, 2013, **49**, 8341; (*b*) J. Kleinwächter and M. Hanack, *J. Am. Chem. Soc.*, 1997, **119**, 10684; (*c*) D. W. DeWulf, J. K. Leland, B. L. Wheeler, A. J. Bard, D. A. Batzel, D. R. Dininny and M. E. Kenney, *Inorg. Chem.*, 1987, **26**, 266; (*d*) B. L. Wheeler, G. Nagasubramanian, A. J. Bard, L. A. Schechtman, D. R. Dininny and M. E. Kenney, *J. Am. Chem. Soc.*, 1984, **106**, 7404; (*e*) E. Ciliberto, K. A. Doris, W. J. Pietro, G. M. Reisner, D. E. Ellis, I. Fragala, F. H. Herbstein, M. A. Ratner and T. J. Marks, *J. Am. Chem. Soc.*, 1984, **106**, 7748.
6 A. Ghosh and M. Ravikanth, *Chem.–Eur. J.*, 2012, **18**, 6386.
7 T. Furuyama, K. Satoh, T. Kushiya and N. Kobayashi, *J. Am. Chem. Soc.*, 2014, **136**, 765.
8 K.-y. Akiba, R. Nadano, W. Satoh, Y. Yamamoto, S. Nagase, Z. Ou, X. Tan and K. M. Kadish, *Inorg. Chem.*, 2001, **40**, 5553.
9 N. Kobayashi, M. Yokoyama, A. Muranaka and A. Ceulemans, *Tetrahedron Lett.*, 2004, **45**, 1755.
10 M. Gouterman, *J. Mol. Spectrosc.*, 1961, **6**, 138.
11 M. Kasha, *Radiat. Res.*, 1963, **20**, 55.
12 L. Huang, P. Zhao, Z. Li, F. Zhang and C.-H. Tung, *J. Phys. Chem. A*, 2008, **112**, 4165.
13 S. E. Maree and T. Nyokong, *J. Porphyrins Phthalocyanines*, 2001, **5**, 782.
14 K. Ishii, H. Itoya, H. Miwa, M. Fujitsuka, O. Ito and N. Kobayashi, *J. Phys. Chem. A*, 2005, **109**, 5781.
15 J. R. Darwent, P. Douglas, A. Harriman, G. Porter and M. C. Richoux, *Coord. Chem. Rev.*, 1982, **44**, 83.